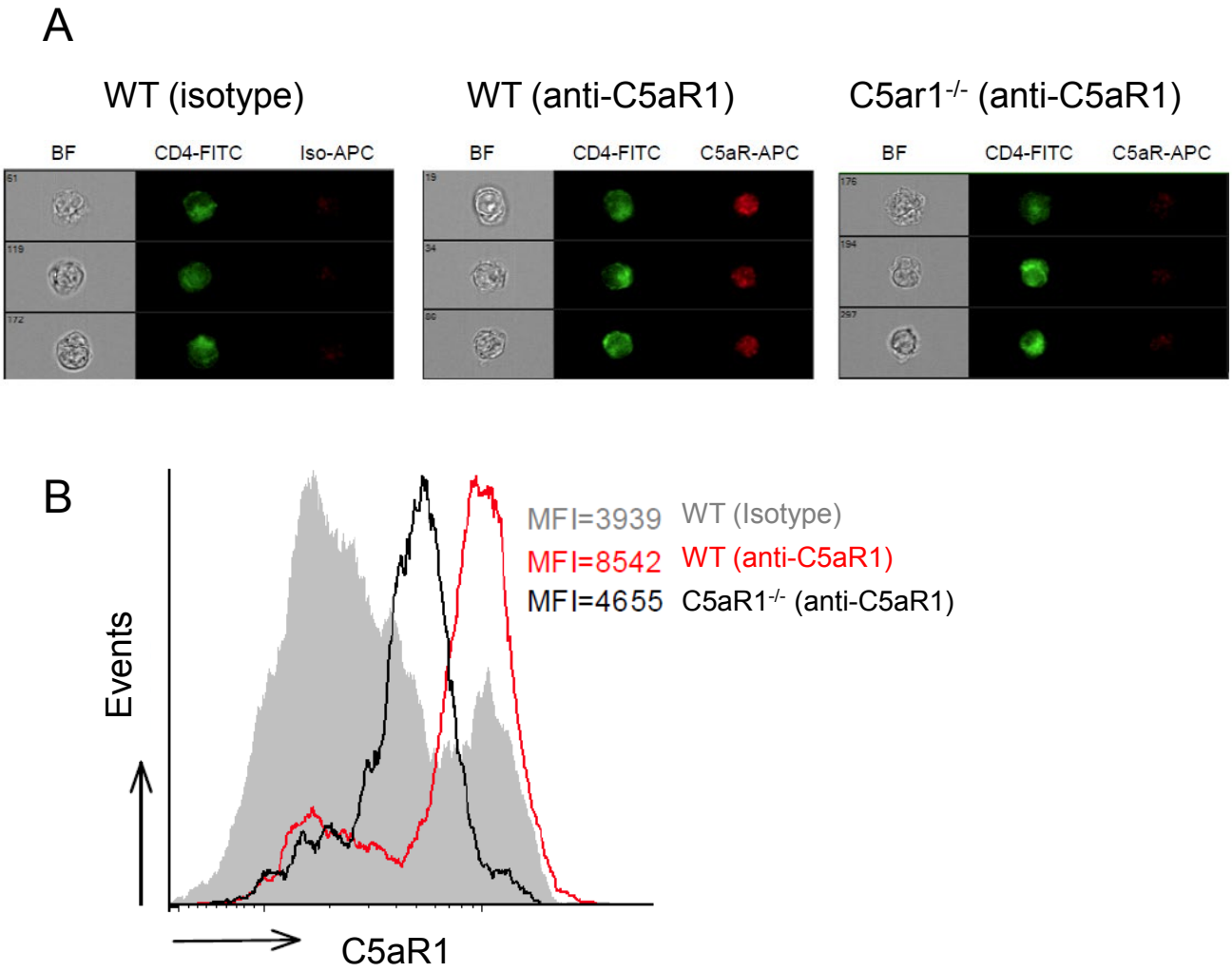

Supplemental Figure 1. Murine T cells express C5aR1. (**A**) Representative Imaging Flow Cytometry images of $CD4^+$ T cells. Splenocytes from wild-type (WT) or *C5ar1*$^{-/-}$ mice were isolated, fixed (PFA 1.6% 10 min 37°C), permeabilized (methanol 10 min 4°C), and stained with an anti-CD4 antibody conjugated to FITC together with an anti-C5aR1 antibody conjugated to APC, or an isotype control. Bright Field, FITC, and APC images were acquired for 10,000 cells per sample using the AMNIS MkII (Millipore Sigma). Pixel-by-pixel compensation was applied using mono-stained samples. (**B**) Distribution of the C5aR1-APC fluorescence intensity integrated across all the pixels in each cell (only $CD4^+$) and summary mean fluorescence intensity (MFI) for WT, *C5ar1*$^{-/-}$ in comparison with isotype.

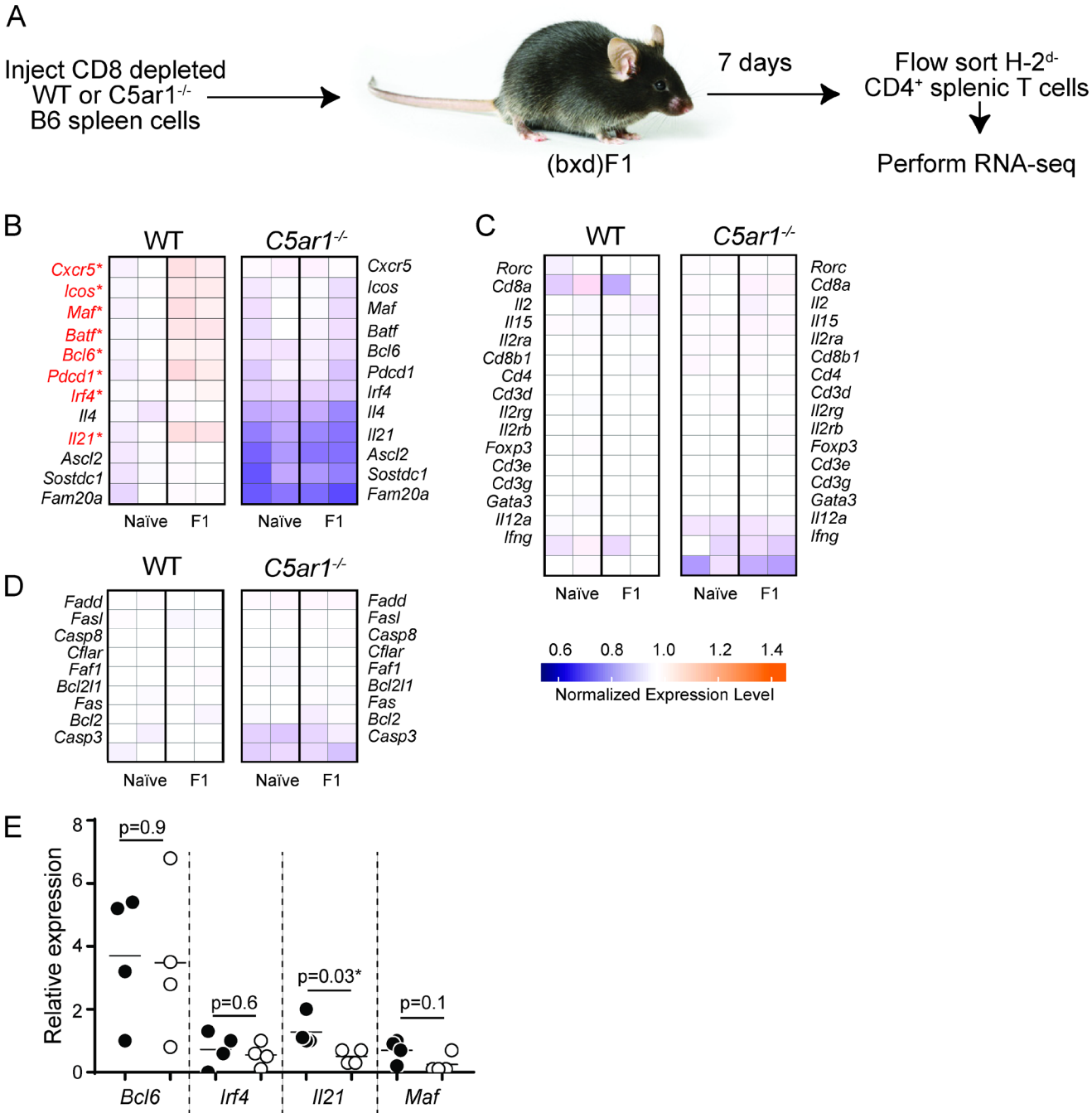

Supplemental Figure 2. C5aR1 modulates T_{FH} differentiation. A. Schematic experimental design. B-D. Gene expression heatmaps for T_{FH} related genes (B), T cell subset genes (C) and survival/apoptosis genes (D) from RNA-seq results, comparing naïve CD4+T cells (left 2 columns) vs CD4+ T cells sorted from F1 mice (right 2 columns) for WT vs *C5ar1*$^{-/-}$ T cells. Differentially upregulated genes are indicated in red (* p<0.05), noting none of the T_{FH}-related genes were significantly upregulated in the *C5ar1*$^{-/-}$ CD4+ after transfer into the F1 recipients. Expression was normalized to the highest expressing gene (in average) in naïve cells for each 4-column panel. E. qRT-PCR results for WT vs C5ar1$^{-/-}$ CD4+ T cells flow sorted on day 7 after transfer into F1 recipients.

Supplemental methods

8 WT (bxd)F1 recipients were injected with CD8-depleted B6 WT (n=4) or *C5ar1*$^{-/-}$ (n=4) CD8-depleted spleen cells. Recipient spleens were harvested on 7d post-transfer and donor CD4^{+} T cells (H-2K^{d-} CD4^{+}) were flow sorted, and RNA was isolated (Qiagen RNAEasy kit, Germantown, MD). Aliquots of each were reversed transcribed for qRT-PCR. The remaining RNA quantities were low so samples were pooled to yield 2 samples of WT CD4^{+} T cells (each comprised of RNA from 2 distinct animals) and 2 samples *C5ar1*$^{-/-}$ CD4^{+} T cells (each comprised of RNA from 2 distinct animals). RNA was also isolate from flow sorted naïve CD4^{+}CD62L^{hi}CD44^{lo} WT (n=2) and *C5ar1*$^{-/-}$ (n=2) mice. DNA was depleted prior to Poly-A selection to improve quality. Single-end sequencing at 51bp read length was performed on a HiSeq 4000 (Illumina, San Diego CA). Good quality reads were aligned to several mouse reference databases including mm10 mouse genome, exon, splicing junction segment using the BWA alignment algorithm, and filtering out reads mapped to a contamination database containing ribosome and mitochondria sequences using BWA alignment algorithm. For each transcript, uniquely-aligned reads to exon and splicing-junction segments with a maximal 2 mis-matches were counted as expression level. Transcripts with an overall low read (<100) across all samples were discarded. Data was then normalized and differentially expressed genes between groups identified utilizing DESeq2. Sequencing data was uploaded to GEO accession number GSE121796 with a release date of Jan 1 2019.

cDNA synthesis, RT, and real-time RT–polymerase chain reaction (PCR) were performed as described [Chun N, et al Am J Transplant 2017;17(11):2810-2819]. PCR products were normalized to the 18S control gene and expressed as fold increase over the mean value of the control group using the DDCt method.